

ESTIMATION OF PARAMETER PROBABILITY DISTRIBUTIONS FOR LITHIUM-ION
BATTERY STRING MODELS USING BAYESIAN METHODS**Luis D. Couto**Department of Engineering Science
University of Oxford
Oxford OX1 3PJ
United Kingdom

Email: luis.coutomendonca@eng.ox.ac.uk

Dong ZhangDepartment of Civil and
Environmental Engineering
University of California, Berkeley
California, 94720

Email: dongzhr@berkeley.edu

Antti AitioDepartment of Engineering Science
University of Oxford
Oxford OX1 3PJ
United Kingdom

Email: antti.aitio@eng.ox.ac.uk

Scott MouraDepartment of Civil and
Environmental Engineering
University of California, Berkeley
California, 94720

Email: smoura@berkeley.edu

David HoweyDepartment of Engineering Science
University of Oxford
Oxford OX1 3PJ
United Kingdom

Email: david.howey@eng.ox.ac.uk

ABSTRACT

This paper addresses the parameter estimation problem for lithium-ion battery pack models comprising cells in series. This valuable information can be exploited in fault diagnostics to estimate the number of cells that are exhibiting abnormal behaviour, e.g. large resistances or small capacities. In particular, we use a Bayesian approach to estimate the parameters of a two-cell arrangement modelled using equivalent circuits. Although our modeling framework has been extensively reported in the literature, its structural identifiability properties have not been reported yet to the best of the authors' knowledge. Moreover, most contributions in the literature tackle the estimation problem through point-wise estimates assuming Gaussian noise using e.g. least-squares methods (maximum likelihood estimation) or Kalman filters (maximum a posteriori estimation). In contrast, we apply methods that are suitable for nonlinear and non-Gaussian estimation problems and estimate the full posterior probability distribution of the parameters. We study how the model structure, available measurements and prior knowledge of the model parameters impact the underlying posterior proba-

bility distribution that is recovered for the parameters. For two cells in series, a bimodal distribution is obtained whose modes are centered around the real values of the parameters for each cell. Therefore, bounds on the model parameters for a battery pack can be derived.

INTRODUCTION

Lithium-ion (Li-ion) batteries are one of the most promising technologies to store energy in a variety of applications, ranging from portable electronics to electric vehicles and smart grids. These batteries benefit from high energy and power density, low self-discharge and long lifetime [1]. However, in contrast to other battery technologies, they need to be properly monitored and controlled to prevent safety hazards [2]. Moreover, since a single battery cell is relatively low voltage, many need to be connected in parallel/series arrangements to form a large scale battery pack. Models of these packs can be seen as interconnected systems with algebraic constraints and dynamic couplings. These features make them more difficult to handle mathematically, and therefore to design monitoring systems for.

There are different approaches to address condition monitoring in batteries, which can be cast as a parameter estimation problem. Two categories can be distinguished, namely approaches that resort to specific experimental techniques, and approaches based on models [3]. The former approaches are computationally simple but they require either a large amount of data or specialized experimental equipment. On the other hand, the latter approaches can be purely data-driven or resort to a specific type of model. Data-driven techniques like support vector machines [4] or neural networks [5] have been used to estimate battery parameters that reflect degradation, such as battery capacity. However, they suffer from requiring big data sets for model training, and they are not constrained by physical principles. Model-based approaches have a more clear interpretation but require skilled domain knowledge to be formulated. Among them, grey-box models like equivalent circuit models (ECM), and more recently white-box models like electrochemical models, are the most widely used frameworks to represent the battery dynamic behaviour. Although electrochemical models are very expressive, they tend to be overparameterized and might be difficult to solve due to model complexity. Overall, ECMs offer a reasonable tradeoff between simplicity and accuracy, even if some degree of physical relevance is lost.

ECMs have been used across the board since the very beginning of battery modeling efforts. When ECMs are concatenated together, they form battery packs. The observability properties of ECMs have been reported several times, either for a single cell [6], cells in parallel [7, 8] and in series [2, 7]. Surprisingly enough, the contributions tackling the parameter identifiability properties of ECMs are limited to recent studies [9, 10], where the structural global identifiability of the 1st-order RC model for a single cell was verified. The parameters of ECMs can be estimated via identification techniques such as nonlinear curve fitting [11, 12], genetic algorithms [13], least-squares methods [14, 15], among others [16]. In contrast to batch model identification, another line of research has focused on real-time state/parameter estimation through Kalman filter-based adaptive filtering techniques [17–19]. All the aforementioned efforts have been devoted to single cells. Results for identifiability and parameter identification of battery packs are more scarce. To the best of the authors' knowledge, structural identifiability of interconnected ECMs for battery packs has only been analyzed in [7]. In the latter work, the identifiability problem is addressed as the observability of the linearized augmented system, while it is known that the observability conditions for nonlinear and linearized systems might differ [6]. On the other hand, the identification problem has only been solved by online state/parameter estimators based on dual Kalman filters [17, 20] and dual nonlinear predictive filter [21].

As described above, most of the parameter estimation schemes used for batteries provide either a point-wise estimation, for example using least squares (maximum likelihood) methods,

or assume a Gaussian distribution for parameter posteriors, for example in Kalman filters. In contrast, other contributions explored more general Bayesian estimation methods, which are less restrictive since they do not assume a priori any form of the conditional density, and they provide confidence bounds for the estimates. Within battery systems, different particle filters (PFs) have been designed for parameter estimation in ECMs [22], as well as state/parameter estimation schemes [23, 24]. Finally, other uses of Bayesian approaches include Markov chain Monte Carlo (MCMC) sampling [25] and uncertainty quantification [26–29] of the model parameters.

In this paper, we use a Bayesian approach to estimate the (possibly non-Gaussian) posterior probability distribution of model parameters in a 2-cell lithium-ion battery described by equivalent-circuit models. The rationale behind allowing non-Gaussianity is that multi-modal distributions can appear when heterogeneous battery cells are considered, especially if they include model parameters far apart in the parameter space. Our contributions are as follows. First, we demonstrate a structural identifiability analysis for an arrangement of two cells in series. Second we estimate the probability distribution of the model parameters, in contrast to the traditional and widely used point-wise estimation. Finally, we analyze the impact of the model structure and parameters on the estimation.

MODELING

We begin by describing the equivalent circuit model (ECM) approach used here to represent the voltage-current dynamics of a single lithium-ion cell. Then, multiple ECMs are interconnected in series to form a string.

Single Battery Cell

An ECM is used to describe the behaviour of the i -th single lithium-ion cell in a string. Figure 1 shows a representation of an ECM, which can be mathematically described by the following continuous-time dynamical system:

$$\dot{x}_i(t) = A_i(\omega_i)x_i(t) + B_i(\omega_i)u_i(t), \quad (1)$$

$$y_i(t) = \text{OCV}_i(x_i(t)) + C_i x_i(t) + D_i(\omega_i)u_i(t), \quad (2)$$

where the state vector is $x_i = [z_i \ V_{ci}]^\top$ consisting of the state of charge (SOC) and the voltage across the R-C pair, respectively, the input u_i is the applied current, the output y_i is the terminal voltage and the parameter vector is defined as $\omega_i = [R_{1i} \ \frac{1}{R_{2i}C_i} \ \frac{1}{C_i}]^\top$. The model parameters consist of an ohmic resistance R_{1i} and the resistance and capacitance of an R-C pair R_{2i}

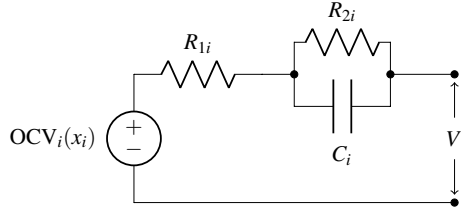


FIGURE 1. EQUIVALENT CIRCUIT MODEL.

and C_i , respectively. The state and input matrices are given by

$$A_i(\omega_i) = \begin{bmatrix} 0 & 0 \\ 0 & -\frac{1}{R_{2i}C_i} \end{bmatrix}, \quad B_i(\omega_i) = \begin{bmatrix} \frac{1}{Q_i} \\ \frac{1}{C_i} \end{bmatrix}, \quad (3)$$

the output function is characterized by the nonlinear open-circuit voltage (OCV) as a function of SOC. Here, a polynomial function

$$\text{OCV}_i(x_i(t)) = p_0 + p_1z_i(t) + p_2z_i(t)^2 + p_3z_i(t)^3 \quad (4)$$

is considered. Finally, $C_i = [0 \ 1]$ and $D_i(\omega_i) = R_{1i}$.

Notice that the ECM in Eqn. (1),(2) has been written in a linear-in-the-parameters form by appropriately grouping the electrical parameters.

String of Cells

When cells are interconnected in series, as depicted in Fig. 2, each cell in the string is represented by an ECM of the form in Eqn. (1),(2) with $i = 1, \dots, N_{\text{cell}}$ for N_{cell} cells in the string. The electrical interconnection of cells in series involves the following Kirchhoff's laws for current and voltage

$$u(t) = u_i(t) \quad \forall i \in \{1, \dots, N_{\text{cell}}\}, \quad (5)$$

$$y(t) = \sum_{i=1}^{N_{\text{cell}}} y_i(t), \quad (6)$$

where u_i and y_i are cell currents and voltages, respectively, and u and y are string currents and voltages, respectively.

Without loss of generality, let us take the case of two cells in series ($N_{\text{cell}} = 2$) to maintain tractability. In that case, the model for the string of cells is given by

$$\dot{x}(t) = f(\omega, x(t), u(t)), \quad (7)$$

$$y(t) = h(\omega, x(t), u(t)), \quad (8)$$

where the string vectors are now the concatenation of the cell vectors, i.e. the state vector is $x = [x_1^T \ x_2^T]^T$ and the parameter

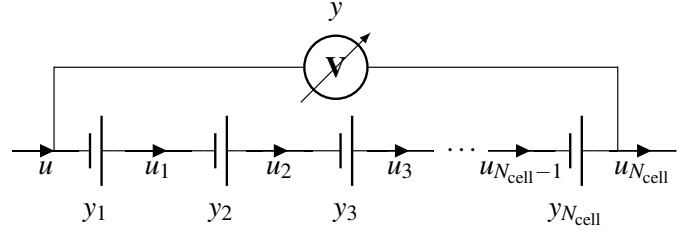


FIGURE 2. SERIES INTERCONNECTION OF BATTERIES.

vector is $\omega = [\omega_1^T \ \omega_2^T]^T$, but the output vector structure depends on what voltage is measured. The nonlinear functions are given by

$$f(\omega, x(t), u(t)) = A(\omega)x(t) + B(\omega)u(t), \quad (9)$$

$$h(\omega, x(t), u(t)) = \text{OCV}(x(t)) + Cx(t) + D(\omega)u(t). \quad (10)$$

In the state equation,

$$A(\omega) = \text{diag}\{A_1(\omega_1), A_2(\omega_2)\}, B(\omega) = [B_1(\omega_1)^T \ B_2(\omega_2)^T]^T,$$

where the diagonal operator $\text{diag}\{\cdot\}$ produces a block-diagonal matrix with the input matrices. In the output equation, two forms can be considered and are compared in this work, namely measuring the string voltage $y_1 + y_2$ with notation

$$\text{OCV}^{[1]}(x(t)) = \text{OCV}_1(x_1(t)) + \text{OCV}_2(x_2(t)) \\ C^{[1]} = [C_1 \ C_2], \quad D^{[1]}(\omega) = D_1(\omega_1) + D_2(\omega_2). \quad (11)$$

or measuring each cell voltages $[y_1 \ y_2]^T$ leading to

$$\text{OCV}^{[2]}(x(t)) = [\text{OCV}_1(x_1(t)) \ \text{OCV}_2(x_2(t))]^T, \\ C^{[2]} = \text{diag}\{C_1, C_2\}, \quad D^{[2]}(\omega) = [D_1(\omega_1) \ D_2(\omega_2)]^T. \quad (12)$$

STRUCTURAL IDENTIFIABILITY

Structural identifiability is a property of the model equations and describes whether or not the model parameters can in principle be uniquely determined from input-output data [30]. Many methods have been proposed to study the structural identifiability of nonlinear systems, such as approaches based on Taylor series expansions, similarity transformations or differential algebra [30, 31]. Here we use differential geometry, which is based on the idea that structural identifiability can be seen as a special case of observability by considering the parameters to be state variables with zero dynamics. We examine the nonlinear (local) observability to assess structural local identifiability.

Let us now introduce the notion of local observability for the system in Eqn. (7),(8) with a time-varying input $\dot{u}(t) \neq 0$.

To improve notational clarity, we write x instead of $x(t)$ and assume that the parameters ω are embedded in the functions, therefore denoting $f(\omega, x(t), u(t))$ and $h(\omega, x(t), u(t))$ as $f(x, u)$ and $h(x, u)$ respectively. In this context, the extended Lie derivative can be defined as [32]

$$L_f h(x, u) = \frac{\partial h(x, u)}{\partial x} f(x, u) + \sum_{j=0}^{j=\infty} \frac{\partial h(x, u)}{\partial u^{(j)}} u^{(j+1)}, \quad (13)$$

where $u^{(j)}$ and $u^{(j+1)}$ denote the j -th and $(j+1)$ -th derivatives of the input, respectively. Higher order Lie derivatives can be calculated as

$$L_f^k h(x, u) = \frac{\partial L_f^{k-1} h(x, u)}{\partial x} f(x, u) + \sum_{j=0}^{j=\infty} \frac{\partial L_f^{k-1} h(x, u)}{\partial u^{(j)}} u^{(j+1)}. \quad (14)$$

Lie derivatives in Eqn. (13),(14) can be used to compute the local observability matrix as

$$\mathcal{O}(x) = \left[\frac{\partial}{\partial x} h(x, u) \quad \frac{\partial}{\partial x} L_f h(x, u) \quad \cdots \quad \frac{\partial}{\partial x} L_f^{n-1} h(x, u) \right]^\top. \quad (15)$$

The system in Eqn. (7)-(8) is locally observable around $x = x_0$ if $\text{rank}(\mathcal{O}(x_0)) = n_x$ where $x \in \mathbb{R}^{n_x}$.

Remark 1. For a constant input $u(t) = \bar{u}$, the extended Lie derivatives in Eqn. (13),(14) simplify to the standard Lie derivatives by cancelling the second terms on the right-hand-side in Eqn. (13),(14).

By augmenting the state of the system with the model parameters with zero dynamics ($\dot{\omega}(t) = 0$), i.e.

$$\bar{x}(t) = \begin{bmatrix} x(t) \\ \omega(t) \end{bmatrix} \quad (16)$$

structural local identifiability can be studied [33]. Similarly as before, the augmented system is locally observable around $\bar{x} = \bar{x}_0$ if $\text{rank}(\mathcal{O}(\bar{x}_0)) = n_{\bar{x}}$ where $n_{\bar{x}} = n_x + n_\omega$ and $\omega \in \mathbb{R}^{n_\omega}$.

BAYESIAN ESTIMATION

We are interested in estimating the posterior distribution of the parameter vector θ conditioned on the observed data y , which is denoted as $p(\theta|y)$. Using Bayes' rule, this distribution is given by

$$p(\theta|y) = \frac{p(y|\theta)p(\theta)}{p(y)} \quad (17)$$

where $p(\theta)$ is the prior distribution of the parameters, $p(y|\theta)$ is the likelihood of the measurements given the parameters and $p(y)$ is a normalization constant defined as

$$p(y) = \int p(y|\theta)p(\theta)d\theta. \quad (18)$$

Unfortunately, this integral is often intractable, but its evaluation is usually avoided by suitable computational algorithms. Therefore, we can actually focus on estimating the marginal posterior distribution of the parameters given by

$$p(\theta|y) \propto p(y|\theta)p(\theta), \quad (19)$$

which is our target distribution.

In parameter estimation it is often convenient to work with the energy function or unnormalized negative log-posterior instead of the marginal likelihood or marginal posterior explicitly [34]. This energy function can be defined as

$$\phi(\theta) \triangleq -\log p(\theta|y) = -\log p(y|\theta) - \log p(\theta), \quad (20)$$

which can be easily evaluated recursively under the Markovian assumption.

First, note that the ECMs in Eqn. (7),(8) can also be written in discrete-time form as

$$x^d(k+1) = A^d(\theta)x^d(k) + B^d(\theta)u^d(k), \quad (21)$$

$$y^d(k) = OCV^d(x^d(k)) + C^d x^d(k) + D^d(\theta)u^d(k) \quad (22)$$

where the superscript d denotes the discrete-time variables. The matrices for the i -th cell are given by

$$A_i^d(\theta_i) = \begin{bmatrix} 1 & 0 \\ 0 & a_i \end{bmatrix}, B_i^d(\theta_i) = \begin{bmatrix} 1 \\ b_i \end{bmatrix}, C_i^d = [0 \quad 1], D_i^d(\theta_i) = c_i, \quad (23)$$

$OCV_i^d(x^d(k))$ is in Eqn. (4) and $\theta_i = [a_i \quad b_i \quad c_i]^\top$, with

$$a_i = e^{\left(-\frac{1}{R_{2i}C_i}\right)}, b_i = R_{2i}(1 - a_i), c_i = R_{1i}, \quad (24)$$

assuming a sampling time $T_s = 1$ s.

The energy function for model in Eqn. (21),(22) is given by

$$\phi(k) = \phi(k-1) + \frac{1}{2} \log |2\pi R| + \frac{1}{2} (y(k) - \hat{y}(k))^\top R^{-1} (y(k) - \hat{y}(k)), \quad (25)$$

where the dependency on θ has been omitted for the sake of simplicity, and where $\phi(0) = -\log p(\theta)$ at $k = 0$. The term R is the estimation error covariance, y is the measured output and \hat{y} is the output predicted by the model with parameters fixed to θ .

By running this algorithm from $k = 0$ up to $k = T$, the full energy function $\phi_T = \phi(T)$ is obtained. Then, sampling methods such as Markov chain Monte Carlo (MCMC) can be used to generate a Monte Carlo approximation of the posterior distribution $p(\theta|y)$. The MCMC is used to draw random variables from a given distribution by exploiting a Markov chain whose stationary distribution is the desired distribution. The advantage of using MCMC to sample from a posterior distribution is that the difficult to compute normalization constant given by Eqn. (18) in Eqn. (17) is not required [34]. Among the different MCMC algorithms, we use an adaptive parallel tempering (APT) algorithm [35]. The APT algorithm allows good mixing with multimodal target distributions π , where conventional Metropolis-Hastings (MH) algorithms [36,37] often fail by getting stuck in one mode. This better mixing within modes is achieved through the tempering of π , i.e. considering auxiliary distributions with density proportional to π^β with $\beta \in (0, 1)$ [35].

The APT algorithm is presented in Tab. 1. In contrast to the MH algorithm based on a single Markov chain, the APT algorithm defines L Markov chains, each of which is associated to a "temperature level" in a temperature ladder. In this way, the APT algorithm is able to explore the parameter space more through the chains at higher temperature and less with the lower temperature chains. Each iteration step of the algorithm can be broken down into three steps. The first step consists of a local exploration that relies on the random walk Metropolis (RWM) algorithm, which is applied to each of the chains $\ell = 1, \dots, L$. This step allows us to keep the most probable parameter candidates while still leaving some room to accept parameters that are less likely. In the second step, the state of two adjacent temperature levels are possibly swapped. The state of the algorithm after the swap is denoted as $\check{\theta}_j^{(\ell)}$, whereas after the random-walk step it is denoted as $\theta_j^{(\ell)}$. While the previous steps are part of traditional parallel tempering algorithms, the third step introduces the adaptation laws. In this step, the temperature parameters $T_j^{(\ell)}$ are continuously updated through a stochastic optimization procedure, where the log-differences between adjacent temperatures $\rho_j^{(\ell)} = \log(T_j^{(\ell+1)} - T_j^{(\ell)})$ is used for the temperature update instead of the temperatures themselves. Then, the random-walk proposal distribution is also adapted at each level through the adaptation of the covariance matrix $\Sigma_j^{(\ell)}$. These steps are repeated for N_{iter} number of iterations.

SIMULATION RESULTS

A simulation study for a string of two lithium-ion cells was carried out to evaluate the performance of the APT algorithm to estimate the underlying (possibly non-Gaussian) probability dis-

TABLE 1. APT ALGORITHM [35].

Initialization: for $j = 0$, $\theta(0)^{(\ell)} = \theta_0^{(\ell)}$, $\Sigma(0)^{(\ell)} = \Sigma_0^{(\ell)}$.

Computation: for $j = 1, 2, \dots, N_{\text{iter}}$ do the following.

Random-walk step: for $\ell = 1, 2, \dots, L$ do

Sampling: draw a candidate point θ^* from the proposal distribution

$$\theta^* \sim q(\theta^* | \theta_{j-1}^{(\ell)}) = \mathcal{N}(\theta^* | \theta_{j-1}^{(\ell)}, \Sigma_j^{(\ell)}).$$

Acceptance probability evaluation:

$$\alpha_j^{(\ell)} = \min \left\{ 1, \exp \left(\frac{1}{T^{(\ell)}} \left(\phi_T(\theta_{j-1}^{(\ell)}) - \phi_T(\theta^*) \right) \right) \frac{q(\theta_{j-1}^{(\ell)} | \theta^*)}{q(\theta^* | \theta_{j-1}^{(\ell)})} \right\}$$

Parameter update: accept candidate point $\theta_j^{(\ell)} = \theta^*$ if

$$\alpha_j^{(\ell)} \geq \mathcal{U}(0, 1).$$

Otherwise $\theta_j^{(\ell)} = \theta_{j-1}^{(\ell)}$. Keep also track of $\phi_T(\theta^{(j)})$.

Swap step: choose a random index $l \in \{1, \dots, L-1\}$ uniformly. Evaluate the acceptance probability

$$\omega_j = \min \left\{ 1, \exp \left(\left(\frac{1}{T^{(l)}} - \frac{1}{T^{(l+1)}} \right) \left(\phi_T(\theta_j^{(l+1)}) - \phi_T(\theta_j^{(l)}) \right) \right) \right\}$$

Accept swap $\check{\theta}_j^{l+1} = \theta_j^l$ and $\check{\theta}_j^l = \theta_j^{l+1}$ if

$$\omega_j \geq \mathcal{U}(0, 1).$$

Do not swap otherwise.

Adapted parameters update: for $\ell = 1, 2, \dots, L$ do

Temperature adaptation step:

$$\rho_j^{(\ell)} = \rho_{j-1}^{(\ell)} + \gamma_{\ell} (\omega_j - \alpha^*).$$

Covariance update:

$$\Gamma_j^{(\ell)} = (1 - \gamma_{\ell}) \Gamma_{j-1}^{(\ell)} + \gamma_{\ell} (\theta_j^{(\ell)} - \mu_{j-1}^{(\ell)}) (\theta_j^{(\ell)} - \mu_{j-1}^{(\ell)})^\top.$$

$$\mu_j^{(\ell)} = (1 - \gamma_{\ell}) \mu_{j-1}^{(\ell)} + \gamma_{\ell} \theta_j^{(\ell)}$$

Level scaling parameters update:

$$\beta_j^{(\ell)} = \beta_{j-1}^{(\ell)} + \gamma_{\ell} (\alpha_j^{(\ell)} - \alpha^*).$$

Adaptive covariance update:

$$\Sigma_j^{(\ell)} = \exp(\beta_j^{(\ell)}) \Gamma_j^{(\ell)}$$

tribution of electrical parameters. We first study the identifiability properties of the 2-cell ECM. Then, the simulation conditions and implementation issues are established. Finally, the effectiveness of the APT algorithm is showcased.

Identifiability Analysis

We use the differential geometry approach explained above to evaluate the structural local identifiability of system in Eqn.

(7),(8). Different cases are considered in terms of input, parameters and output. First, two inputs are evaluated, namely constant input $u(t) = \bar{u}$ and time-varying input $\dot{u}(t) \neq 0$. Secondly, the parameter vectors of the two cells might be equal $\omega_1 = \omega_2$ or different $\omega_1 \neq \omega_2$. Finally, the measured output can consist of the local voltages $[y_1 \ y_2]^\top$ or the total voltage $y = y_1 + y_2$.

Under constant input current $\dot{u}(t) = 0$, the model in Eqn. (7),(8) is always structurally unidentifiable (i.e. $\text{rank}(\mathcal{O}(x_0)) < n_{\bar{x}}$) regardless of the parametric structure or measured outputs. Therefore, from now on we focus on time-varying inputs $\dot{u}(t) \neq 0$. All these remaining cases are summarized in Tab. 2, together with the obtained identifiability results. When the two voltage measurements are considered, the system model in Eqn. (7),(8) is structurally locally identifiable ($\text{rank}(\mathcal{O}(x_0)) = n_{\bar{x}}$). But when the string voltage is measured, structural identifiability is lost ($\text{rank}(\mathcal{O}(x_0)) < n_{\bar{x}}$).

TABLE 2. IDENTIFIABILITY OF THE ECM IN EQN. (7),(8).

Parameters	Output	$n_{\bar{x}}$	$\text{rank}(\mathcal{O}(x_0))$
$\omega_1 = \omega_2$	$[y_1 \ y_2]^\top$	7	7
$\omega_1 = \omega_2$	$y_1 + y_2$	7	6
$\omega_1 \neq \omega_2$	$[y_1 \ y_2]^\top$	10	10
$\omega_1 \neq \omega_2$	$y_1 + y_2$	10	8

Implementation of the APT Algorithm

Based on the identifiability analysis results shown in Tab. 2, we know that we need at least a non-constant excitation $\dot{u}(t) \neq 0$ for the model to be identifiable. With respect to the parameters of each cell, we do not have control over them in a real battery. The heterogeneity of cells depends on the manufacturer and the condition of the batteries themselves. We also know that it is preferable to measure the local voltages of the two cells in the string. Now, we exploit these insights to properly formulate the probabilistic model that is used by the APT algorithm to estimate the ECM parameters.

In the following, we set up the series of experiments to be carried out in simulation as well as the APT algorithm for the specific problem at hand, i.e. the estimation of the probability distribution of the ECM parameters for two lithium-ion battery cells connected in series. A driving cycle is used as input current profile (Fig. 3). Even if this input becomes zero during some specific time intervals in which the structural observability is lost, such periods are scarce and observability can be recovered quickly as soon as $u \neq 0$. The model for simulation of the two battery cells in series correspond to the discrete-time model in Eqn. (21),(22). The parameter values for each ECM are reported in Tab. 3.

The different cases considered are shown in Tab. 4. Recall that the parameter vector is $\theta = [\theta_1^\top \ \theta_2^\top]^\top$ with $\theta_i = [a_i \ b_i \ c_i]^\top, i \in \{1, 2\}$ defined in Eqn. (24). Two main cases for

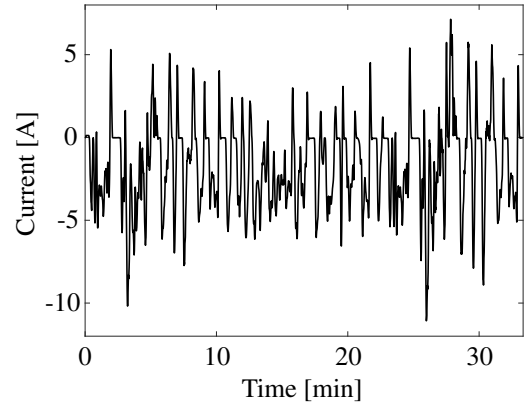


FIGURE 3. APPLIED UDDS DRIVING CYCLE.

TABLE 3. ECM SIMULATION PARAMETERS.

Parameter	Cell 1	Cell 2
R_1	0.005	0.015
R_2	0.0014	0.0047
C_2	2470.3	923.4
Q	3600	3600
p_i^\dagger	{3.4707, 1.6112, -2.6287, 1.7175}	

[†]Both cells share the same OCV function, with $i = 0, \dots, 3$.

the model structure are considered in simulation, namely the two cells differ in one (case 1) or two (case 2) parameters. These cases are further subdivided into:

- cases 1.1 and 2.1, where the parameter to be estimated is chosen to be c , and the structure of the model (i.e. the degree of equivalence between cells) is studied;
- cases 1.1 and 1.2, where the nature of the parameters to be estimated is different, since b and c are input coefficients in the state and output equations, respectively;
- cases 2.1, 2.2 and 2.3, where the model structure is specified to be $b_1 \neq b_2$ and $c_1 \neq c_2$, and the parameters to be estimated are studied (i.e. the structure of the estimator).

Note that for the sake of simplicity, only parameters b and c are subject to parameter estimation, while $a_1 = a_2$.

We devised a parameter identification scheme that provides us with the underlying probability distribution associated with each ECM parameter for a battery pack described by Eqn. (21),(22). However, instead of considering directly the model in Eqn. (21),(22), we reformulated the model in two ways:

- The parameter identification setup consists of assuming the same parameter vector $\hat{\theta} = [\hat{a} \ \hat{b} \ \hat{c}]^\top$ for all cells in the string, instead of taking a specific point value θ_i for each i -th cell. In other words, each component of the parameter vector $\hat{\theta}$ is

TABLE 4. CONSIDERED SIMULATION CASES

Case	$b_1 \stackrel{?}{=} b_2$	E^\dagger	$c_1 \stackrel{?}{=} c_2$	E
1.1	=	-	\neq	\times
1.2	\neq	\times	=	-
2.1	\neq	-	\neq	\times
2.2	\neq	\times	\neq	-
2.3	\neq	\times	\neq	\times

[†]The entries in column E marked with \times mean that a particular parameter is estimated.

described by a distribution that could be non-Gaussian. Note that the proposed parameter vector $\hat{\theta} \in \mathbb{R}^3$, which contrasts with $\theta \in \mathbb{R}^6$ in model Eqn. (21),(22).

2. Instead of directly dealing with the discrete-time model parameters θ as in Eqn. (24), we rewrite the parameter vector $\hat{\theta}$ introduced in point 1 above in terms of the variables $\Delta_\theta = [\Delta_a \ \Delta_b \ \Delta_c]^\top$ that perturb the parameter around a nominal value $\bar{\theta}$, i.e. $\hat{\theta} = \Delta_\theta \bar{\theta}$ (this product is understood component-wise). Normalized parameters Δ_θ are better conditioned than true parameters whose values might differ in orders of magnitude.

We aim at identifying Δ_θ whereas $\bar{\theta}$ is known. To make these two notions more explicit, we can reformulate the model in Eqn. (21),(22) accordingly as

$$x^d(k+1) = A^d(\Delta_\theta \bar{\theta})x^d(k) + B^d(\Delta_\theta \bar{\theta})u^d(k), \quad (26)$$

$$y^d(k) = OCV^d(x^d(k)) + C^d x^d(k) + D^d(\Delta_\theta \bar{\theta})u^d(k) \quad (27)$$

Remark 2. *These simplifications allow us to directly estimate a (possibly non-Gaussian) probability distribution associated to the ECM parameters for a given battery pack. If the battery pack has e.g. 100 cells, then the resulting estimation for e.g. the series resistance R_1 represents the probability distribution associated with the resistance of the pack. This information can be further exploited for pack SOH estimation while having an idea of the proportion of cells that are in the most critical condition.*

The APT algorithm is designed on the basis of Eqn. (26),(27). In all the experiments, the estimation algorithm was set up with the conditions presented next. In the general case of N_{cell} battery cells connected in series, the likelihood function is selected to be multimodal, which takes the form

$$p(y|\theta) = \frac{1}{N_{\text{cell}}} \sum_{i=1}^{N_{\text{cell}}} \frac{1}{|2\pi R_i|^{1/2}} \exp\left(-\frac{1}{2}(y_i - \hat{y}_i)^\top R_i^{-1}(y_i - \hat{y}_i)\right). \quad (28)$$

The subscript i represents each i -th battery cell. This likelihood function in Eqn. (28) is used in the energy function in Eqn.

(25). For the case of two cells in series, $N_{\text{cell}} = 2$ and the covariance of the estimation error is $R = 10^{-4}I_2$. The nominal parameter values $\bar{\theta}$ in the model Eqn. (26),(27) are set to the mean values of the real discrete-time parameters $\bar{\theta}_i$ for the considered cells. The parameters Δ_θ to be estimated by the APT algorithm are initialized with $\Delta_\theta(0) = \Delta_{\theta,0}1_{n_e \times 1}$, where n_e is the number of parameters to be estimated and $\Delta_{\theta,0} = 1.6$. The algorithm was initialized with a uniform prior probability distribution $p(\Delta_\theta) = \mathcal{U}(u1_{1 \times n_e}, \bar{u}1_{1 \times n_e})$, $u = 0$, $\bar{u} = 3$. These bounds are selected because we know that the parameters are positive and we add approximately 90% of uncertainty to the initial parameter value. The initial values for the adapted parameters are: covariance $\Sigma_0^{(\ell)} = \sigma_0^2 I_{n_e}$, $\sigma_0^2 = 10^{-6}$, temperature difference $\rho_0^{(\ell)} = 1$ and scalings $\beta_0^{(\ell)} = 1$. The step-size sequences are $\gamma_k = (j+1)^{-0.6}$, $k \in \{1, 2, 3\}$. A total of 5000 MCMC iterations were considered.

Results & Discussion

The estimation results for case 1 are shown in Fig. 4. The state of charge and the voltage response of cell 1 are depicted in Fig. 4(A) and (D), respectively. It can be seen that the drive cycle has been scaled to cover a wide range of SOC. Figures 4(B),(E) and Figs. 4(C),(F) show the estimation results for parameters Δ_c (case 1.1) and Δ_b (case 1.2), respectively. Figures 4(B),(C) show the evolution of the estimated parameter for each iteration, whereas Figs. 4(E),(F) show the resulting probability distributions. The two dashed black lines in the plots represent the true parameters, whereas the solid green line in the bottom plots correspond to the uniform prior probability distribution. These plot conventions are maintained for the other plots. Two output equation structures are also compared here, namely when the two cell voltages are measured (blue curves) and when only the total voltage is measured (red curves). Focusing on the two voltage measurements first, the results for Δ_c (Figs. 4(B),(E)) show a bimodal distribution with the two modes centered around the true parameter values, and the results for Δ_b (Figs. 4(C),(F)) show a unimodal distribution centered around 1, which also corresponds to the average value of the two real parameters.

Notice that for both parameters Δ_c and Δ_b , the same considerations apply: the simulations were done for two cells in series with different parameters (approximately 0.5 and 1.5), and both parameters are input coefficients, the former in the output equation and the latter in the state equation. However, the shape of their associated probability distribution is different. Even if a bimodal distribution was also expected for Δ_b , it is suppressed in favor of a unimodal distribution. Since this model has been verified to be structurally identifiable, these results only suggest that the energy function is maximized around the mean value of the true parameters instead of the real parameters. Therefore, the type of parameter to be estimated influences the associated probability distribution.

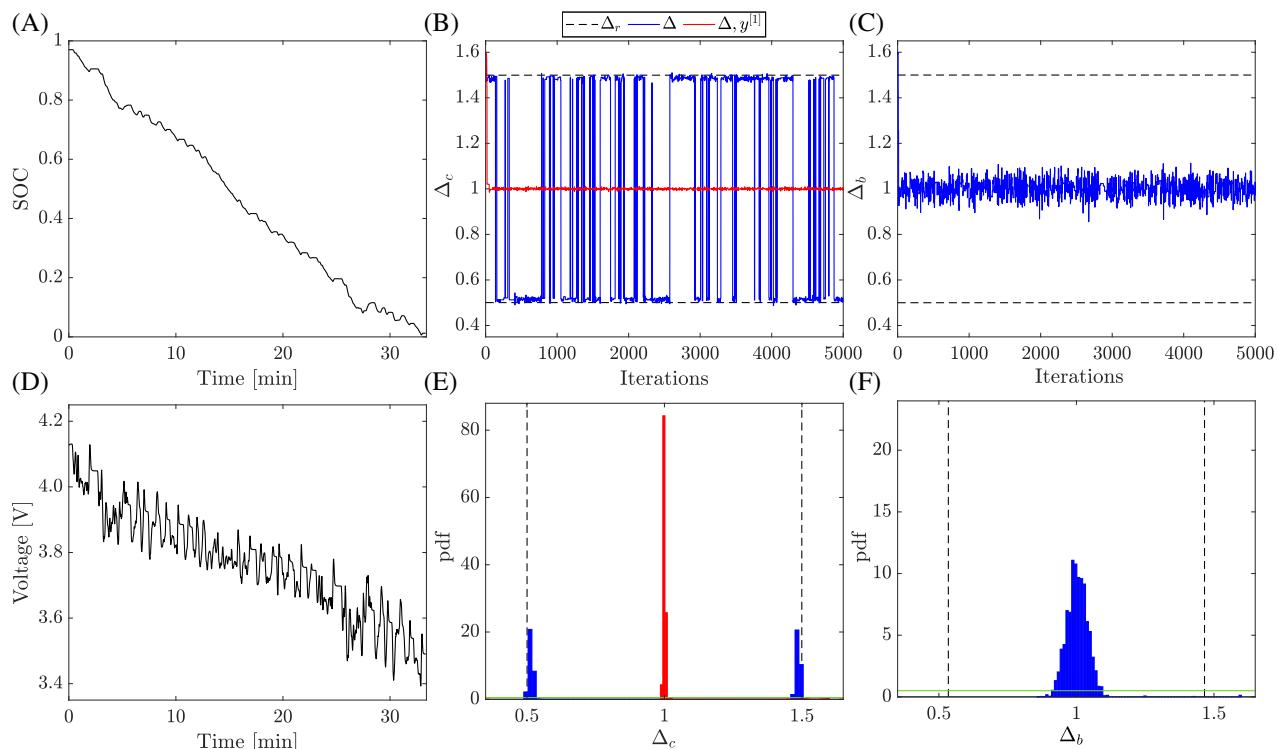


FIGURE 4. PARAMETER IDENTIFICATION RESULTS USING THE APT ALGORITHM FOR CASE 1. (A) CURRENT, MARKOV CHAIN FOR (B) Δ_c and (C) Δ_b , (D) VOLTAGE, PROBABILITY DISTRIBUTION FOR (E) Δ_c and (F) Δ_b .

When the total voltage of the string is measured (red curve in Fig. 4(B) and distribution in Fig. 4(E)), then a unimodal distribution is obtained for Δ_c , which is centered around 1 (the average value of the true two parameters). Therefore, the measured signals impact the underlying probability distribution obtained from parameter estimation, which in this case could be ascribed to identifiability issues. From now on, the two cell voltages are measured.

Now we look at case 2. On the one hand and due to space constraints, the cases 2.1 and 2.2 are not plotted here but the results are equivalent to the ones obtained for cases 1.1 and 1.2, respectively. This fact confirms that the model structure does not affect the shape of the estimated probability distribution. On the other hand, Fig. 5 shows the estimation results for case 2.3. Figures 5(A),(D) and Figs. 5(B),(E) depict the results for parameters Δ_c and Δ_b , respectively. Figures 5(D),(E) show the marginal posterior distribution for each parameter. Figure 5(C) portrays the simulated points of the tempered distributions corresponding to the joint distribution for both Δ_c and Δ_b parameters, where the temperature levels from 1 to 5 are shown from top to bottom plots. Notice that a more diffuse distribution is obtained at higher temperature levels (bottom plot, level 5) whereas clear peaks appear at lower temperatures (top plot, level 1). In this case, when both parameters Δ_c and Δ_b are estimated together, they exhibit bimodality, even though when only Δ_b is estimated (it is assumed

that Δ_c is known), a unimodal distribution appears. This result implies that the prior knowledge (which parameters are known) as well as the structure of the estimator (which parameters are estimated) impact the final estimation results to the extent that wrong estimates might be obtained under reckless assumptions. Again, the APT algorithm chooses one distribution over another by maximizing the energy function.

CONCLUSIONS

The parameters of a lithium-ion battery system with 2 cells in series have been estimated. Firstly, structural identifiability was undertaken for cells in series. The analysis shows the model to be structurally locally identifiable if the input current is time-varying and the voltage of each cell is measured. Then, a Bayesian approach was used to estimate the underlying probability distributions characterizing the model parameters. In general, we found that the shape (unimodal or bimodal) of the probability density of the posterior distribution depends on whether some parameters are known or should be estimated, as well as the type of parameters (where they appear in the model) to be estimated. Moreover, the model structure, understood as the degree of equivalence between the two cells, has little impact on the estimation results. Future work will be devoted to increasing the number of cells and estimating the probability distribution of the battery pack as a whole using the proposed identification

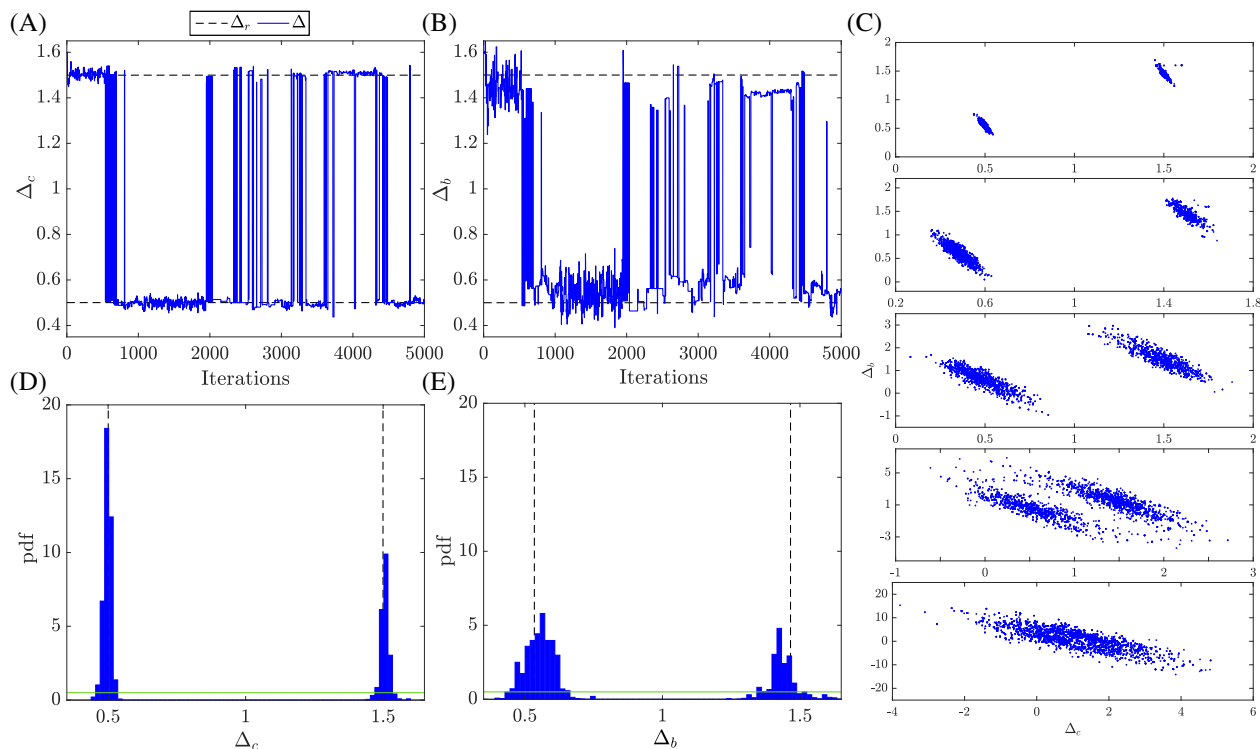


FIGURE 5. PARAMETER IDENTIFICATION RESULTS USING THE APT ALGORITHM FOR CASE 2. MARKOV CHAIN FOR (A) Δ_c and (B) Δ_b , (C) TEMPERATURE LEVELS FROM 1 (TOP) TO 5 (BOTTOM), PROBABILITY DISTRIBUTION FOR (D) Δ_c AND (E) Δ_b .

framework.

ACKNOWLEDGMENT

Luis D. Couto would like to thank the Wiener-Anspach Foundation for its financial support.

REFERENCES

- [1] Chaturvedi, N. A., Klein, R., Christensen, J., Ahmed, J., and Kojic, A., 2010. "Algorithms for advanced battery-management systems". *IEEE Control Systems*, **30**(3), pp. 49–68.
- [2] Lin, X., and Stefanopoulou, A. G., 2015. "Analytic bound on accuracy of battery state and parameter estimation". *Journal of The Electrochemical Society*, **162**(9), pp. A1879–A1891.
- [3] Berecibar, M., Gandiaga, I., Villarreal, I., Omar, N., Van Mierlo, J., and Van den Bossche, P., 2016. "Critical review of state of health estimation methods of Li-ion batteries for real applications". *Renewable and Sustainable Energy Reviews*, **56**, pp. 572–587.
- [4] Yang, D., Wang, Y., Pan, R., Chen, R., and Chen, Z., 2018. "State-of-health estimation for the lithium-ion battery based on support vector regression". *Applied Energy*, **227**, pp. 273–283.
- [5] Yang, D., Wang, Y., Pan, R., Chen, R., and Chen, Z., 2017. "A neural network based state-of-health estimation of lithium-ion battery in electric vehicles". *Energy Procedia*, **105**, pp. 2059–2064.
- [6] Zhao, S., Duncan, S. R., and Howey, D. A., 2017. "Observability analysis and state estimation of lithium-ion batteries in the presence of sensor biases". *IEEE Transactions on Control Systems Technology*, **25**(1), pp. 326–333.
- [7] Rausch, M., Streif, S., Pankiewicz, C., and Findeisen, R., 2013. "Nonlinear observability and identifiability of single cells in battery packs". In IEEE International Conference on Control Applications, pp. 401–406.
- [8] Zhang, D., Couto, L. D., Benjamin, S., Zeng, W., Coutinho, D. F., and Moura, S. J., 2020. "State of charge estimation of parallel connected battery cells via descriptor system theory". In American Control Conference (to appear).
- [9] Alavi, S. M. M., Mahdi, A., Payne, S. J., and Howey, D. A., 2017. "Identifiability of generalized randles circuit models". *IEEE Transactions on Control Systems Technology*, **25**(6), pp. 2112–2120.
- [10] Grandjean, T. R. B., McGordon, A., and Jennings, P. A., 2017. "Structural identifiability of equivalent circuit models for Li-ion batteries". *Energies*, **10**(1), p. 90.
- [11] Eltoumi, F., Badji, A., Becherif, M., and Ramadan, H. S., 2018. "Experimental identification using equivalent circuit model for lithium-ion battery". *International Journal of Emerging Electric Power Systems*, **19**(3), p. 1.

- [12] Pei, Z., Xiaoxu Zhao, Huimei Yuan, Z. P., and Wu, L., 2018. "An equivalent circuit model for lithium battery of electric vehicle considering self-healing characteristic". *Journal of Control Science and Engineering*, **2018**, p. 5179758.
- [13] He, H., and Xiong, R.; Fan, J., 2011. "Evaluation of lithium-ion battery equivalent circuit models for state of charge estimation by an experimental approach". *Energies*, **4**, pp. 582–598.
- [14] Tian, N., Wang, Y., Chen, J., and Fang, H., 2017. "On parameter identification of an equivalent circuit model for lithium-ion batteries". In *IEEE Conference on Control Technology and Applications*, pp. 187–192.
- [15] Wen, F., Duan, B., Zhang, C., Zhu, R., Shang, Y., and Zhang, J., 2019. "High-accuracy parameter identification method for equivalent-circuit models of lithium-ion batteries based on the stochastic theory response reconstruction". *Electronics*, **8**(8), p. 834.
- [16] Madani, S. S., Schaltz, E., and Kær, S. K., 2018. "A review of different electric equivalent circuit models and parameter identification methods of lithium-ion batteries". *ECS Transactions*, **87**(1), pp. 23–37.
- [17] Plett, G. L., 2004. "Extended Kalman filtering for battery management systems of LiPB-based HEV battery packs: Part 3. State and parameter estimation". *Journal of Power Sources*, **134**(2), pp. 277–292.
- [18] Xiong, R., Sun, F., Gong, X., and Gao, C., 2014. "A data-driven based adaptive state of charge estimator of lithium-ion polymer battery used in electric vehicles". *Applied Energy*, **113**, pp. 1421–1433.
- [19] Guo, X., Kang, L., Yao, Y., Huang, Z., and Li, W., 2016. "Joint estimation of the electric vehicle power battery state of charge based on the least squares method and the Kalman filter algorithm". *Energies*, **9**(2), p. 100.
- [20] Zhang, X., Wang, Y., Yang, D., and Chen, Z., 2016. "An on-line estimation of battery pack parameters and state-of-charge using dual filters based on pack model". *Energy*, **115**, pp. 219–229.
- [21] Hua, Y., Cordoba-Arenas, A., Warner, N., and Rizzoni, G., 2015. "A multi time-scale state-of-charge and state-of-health estimation framework using nonlinear predictive filter for lithium-ion battery pack with passive balance control". *Journal of Power Sources*, **280**(0), pp. 293–312.
- [22] Saha, B., Goebel, K., Poll, S., and Christophersen, J., 2009. "Prognostics methods for battery health monitoring using a Bayesian framework". *Instrumentation and Measurement, IEEE Transactions on*, **58**(2), pp. 291–296.
- [23] Schwunk, S., Armbruster, N., Straub, S., Kehl, J., and Vetter, M., 2013. "Particle filter for state of charge and state of health estimation for lithium-iron phosphate batteries". *Journal of Power Sources*, **239**, pp. 705–710.
- [24] Xu, W., Xu, J., and Yan, X., 2020. "Lithium-ion battery state of charge and parameters joint estimation using cubature Kalman filter and particle filter". *Journal of Power Electronics*, **20**(1), pp. 292–307.
- [25] Aitio, A., Marquis, S. G., Ascencio, P., and Howey, D., 2020. "Bayesian parameter estimation applied to the Li-ion battery single particle model with electrolyte dynamics". *arXiv2001.09890v1*.
- [26] Ramadesigan, V., Chen, K., Burns, N. A., Boovaragavan, V., Braatz, R. D., and Subramanian, V. R., 2011. "Parameter estimation and capacity fade analysis of lithium-ion batteries using reformulated models". *Journal of The Electrochemical Society*, **158**(9), pp. A1048–A1054.
- [27] Tong, W., Koh, W. Q., Birgersson, E., Mujumdar, A. S., and Yap, C., 2015. "Correlating uncertainties of a lithium-ion battery – A Monte Carlo simulation". *International Journal of Energy Research*, **39**(6), pp. 778–788.
- [28] López C, D. C., Wozny, G., Flores-Tlacuahuac, A., Vasquez-Medrano, R., and Zavala, V. M., 2016. "A computational framework for identifiability and ill-conditioning analysis of lithium-ion battery models". *Industrial & Engineering Chemistry Research*, **55**(11), pp. 3026–3042.
- [29] Sethurajan, A., Krachkovskiy, S., Goward, G., and Protas, B., 2019. "Bayesian uncertainty quantification in inverse modeling of electrochemical systems". *Journal of Computational Chemistry*, **40**(5), pp. 740–752.
- [30] Villaverde, A., and Barreiro, A., 2016. "Identifiability of large nonlinear biochemical networks". *MATCH Communications in Mathematical and in Computer Chemistry*, **76**, pp. 259–296.
- [31] Walter, E., and Pronzato, L., 1997. *Identification of Parametric Models*. Springer-Verlag London.
- [32] F., V. A., Nikolaos, T., and R., B. J., 2019. "Full observability and estimation of unknown inputs, states and parameters of nonlinear biological models". *J. R. Soc. Interface*, **16**.
- [33] Villaverde, A. F., 2019. "Observability and structural identifiability of nonlinear biological systems". *Complexity*, **2019**, p. 12.
- [34] Särkkä, S., 2013. *Bayesian Filtering and Smoothing*, Vol. 3. Cambridge University Press.
- [35] Miasojedow, B., Moulines, E., and Vihola, M., 2013. "An adaptive parallel tempering algorithm". *Journal of Computational and Graphical Statistics*, **22**(3), pp. 649–664.
- [36] Metropolis, N., Rosenbluth, A. W., Rosenbluth, M. N., Teller, A. H., and Teller, E., 1953. "Equation of state calculations by fast computing machines". *The Journal of Chemical Physics*, **21**(6), pp. 1087–1092.
- [37] Hastings, W. K., 1970. "Monte Carlo sampling methods using Markov chains and their applications". *Biometrika*, **57**(1), pp. 97–109.